Plant, Cell and Environment (2009) doi: 10.1111/j.1365-3040.2009.01959.x

High-frequency field measurements of diurnal carbon isotope discrimination and internal conductance in a semi-arid species, *Juniperus monosperma*

CHRISTOPHER P. BICKFORD[1], NATE G. MCDOWELL[3], ERIK B. ERHARDT[2] & DAVID T. HANSON[1]

[1]Department of Biology, MSC03-2020 and [2]Department of Mathematics and Statistics, MSC03-2150, University of New Mexico, Albuquerque, NM 87131, USA and [3]Earth and Environmental Sciences Division, MS-J495, Los Alamos National Laboratory, Los Alamos, NM 87544, USA

ABSTRACT

We present field observations of carbon isotope discrimination (Δ) and internal conductance of CO_2 (g_i) collected using tunable diode laser spectroscopy (TDL). Δ ranged from 12.0 to 27.4‰ over diurnal periods with daily means from 16.3 ± 0.2‰ during drought to 19.0 ± 0.5‰ during monsoon conditions. We observed a large range in g_i, with most estimates between 0.04 and 4.0 μmol m^{-2} s^{-1} Pa^{-1}. We tested the comprehensive Farquhar, O'Leary and Berry model of Δ (Δ_{comp}), a simplified form of Δ_{comp} (Δ_{simple}) and a recently suggested amendment ($\Delta_{revised}$). Sensitivity analyses demonstrated that varying g_i had a substantial effect on Δ_{comp}, resulting in mean differences between observed Δ (Δ_{obs}) and Δ_{comp} ranging from 0.04 to 9.6‰. First-order regressions adequately described the relationship between Δ and the ratio of substomatal to atmospheric CO_2 partial pressure (p_i/p_a) on all 3 d, but second-order models better described the relationship in July and August. The three tested models each best predicted Δ_{obs} on different days. In June, Δ_{simple} outperformed Δ_{comp} and $\Delta_{revised}$, but incorporating g_i and all non-photosynthetic fractionations improved model predictions in July and August.

Key-words: decarboxylation; Farquhar model; mesophyll conductance; p_i/p_a.

INTRODUCTION

Stable carbon isotope analyses have a long history in plant biology that includes differentiation of photosynthetic pathways (Smith & Epstein 1971), development of physiological theory of carbon isotope fractionation (O'Leary 1981; Farquhar, O'Leary & Berry 1982), crop improvement (Farquhar & Richards 1984), ecological studies (Ehleringer 1993; Brooks *et al.* 1997), ecosystem process studies (Bowling *et al.* 2002; McDowell *et al.* 2004) and biosphere–atmosphere interactions (Yakir 2003; Randerson *et al.* 2006). The biological and physical discrimination against the $^{13}C^{16}O_2$ isotopologue during diffusion and carboxylation is a strong regulator of the isotopic signature of ecosystem exchange with the atmosphere as it largely determines the ^{13}C composition of the substrate pool, which supplies respiratory activity (Barbour *et al.* 2005; Knohl *et al.* 2005; Bowling, Pataki & Randerson 2008). The transfer of this signature throughout the ecosystem provides a useful signal to partition components of ecosystem carbon exchange and aids in carbon cycle modelling (Ciais *et al.* 1995; Tu & Dawson 2005; McDowell *et al.* 2008a).

A substantial body of literature describing a linear relationship between leaf carbon isotope discrimination (Δ) and the ratio of internal to atmospheric CO_2 partial pressure (p_i/p_a) has accumulated in the last three decades (Farquhar *et al.* 1982b; Brugnoli *et al.* 1988; Farquhar, Ehleringer & Hubick 1989; Ehleringer, Phillips & Comstock 1992; Brugnoli & Farquhar 2000). The p_i/p_a ratio is useful because it succinctly describes the dominant physical and biochemical constraints to photosynthesis. Similarly, the linear relationship between Δ and p_i/p_a observed in previous studies emphasizes the importance of stomatal conductance and biochemistry in Δ. The full model of Δ developed by Farquhar *et al.* (1982) also accounts for other factors such as internal conductance of CO_2 from stomatal cavities to sites of carboxylation (g_i) and apparent isotopic fractionations associated with the decarboxylation processes of day respiration and photorespiration (Δ_{ef}), as well as other diffusion-related fractionations. Recent evidence suggests that g_i and Δ_{ef} are sensitive to environmental factors that vary diurnally (Bernacchi *et al.* 2002; Ghashghaie *et al.* 2003; Warren, Livingston & Turpin 2004), but their role in the variation in Δ observed in a field setting remains poorly understood.

Temperature and water stress have been shown to impact g_i. Bernacchi *et al.* (2002) found that temperature regulated g_i within the biologically significant range of 10–40 °C in tobacco, a finding supported in work presented by Yamori *et al.* (2006) and Warren & Dreyer (2006) using different species. Water stress also reduces g_i, as demonstrated experimentally in *Pseudotsuga* seedlings (Warren *et al.* 2004) and *Olea* (Diaz-Espejo, Nicolás & Fernandez 2007) and in a comprehensive field study using *Quercus* and *Fraxinus* (Grassi & Magnani 2005). Recently, a strong

Correspondence: C. P. Bickford. Fax: +1 505 277 0304; e-mail: bickford@unm.edu

linkage between aquaporin function and g_i was established (Flexas *et al.* 2006; Uehlein *et al.* 2008), providing a possible mechanism for rapid variation in g_i in response to a multitude of environmental factors, as has been demonstrated in response to CO_2 concentration (Flexas *et al.* 2007). While seasonal changes in g_i have been documented in a field setting (Grassi & Magnani 2005; Diaz-Espejo *et al.* 2007), diurnal variation in g_i has not yet been reported.

The influence of environmental factors on Δ_{ef} is less well known. Temperature and light have been shown to influence day respiration and photorespiration, both of which affect CO_2 evolution within a leaf (Brooks & Farquhar 1985; Kozaki & Takeba 1996; Atkin *et al.* 2000, 2005). The apparent fractionation associated with day respiration (e) and photorespiration (f) are each the result of biochemical reactions that may be subject to environmental control (Ghashghaie *et al.* 2003). A consistent enrichment of 6‰ in the dark respired $^{13}C/^{12}C$ ratio ($\delta^{13}C_{resp}$) of CO_2 compared to sucrose of droughted and control *Phaseolus* leaves has been observed (Duranceau *et al.* 1999). Such respiratory enrichment has been shown to depend on species and on plant water status (Ghashghaie *et al.* 2001), temperature (Tcherkez *et al.* 2003), and light exposure (Barbour *et al.* 2007a). Estimates of e have largely been inferred from studies of dark respiration, but recent evidence suggests these dark respiration fractionations may not be representative of day respiratory fractionation (Tcherkez *et al.* 2008). Field observations of the diurnal patterns of the cumulative fractionation associated with respiratory and photorespiratory processes, estimated here in Δ_{ef}, may allow us to better understand the influence of environmental factors on this component of Δ.

In recent years, advances in optical systems utilizing tunable diode laser spectroscopy (TDL) have simplified high-frequency measurements of the abundance of individual isotopologues $^{13}C^{16}O_2$, $^{12}C^{16}O_2$ and $^{12}C^{18}O^{16}O$ in ecosystem studies (Bowling *et al.* 2003; Griffis *et al.* 2004; McDowell *et al.* 2008a) and leaf-scale studies in greenhouse settings (Barbour *et al.* 2007a,b) Similar TDL leaf-scale measurements can now be attempted in a field setting. The objectives of this study were to (1) examine the temporal variation in Δ, $\delta^{13}C_{resp}$, g_i and Δ_{ef} under ambient field conditions; (2) test the hypothesis that g_i varies across the day; (3) test the hypothesis that Δ varies linearly in response to shifts in p_i/p_a under field conditions; (4) test the influence of g_i in a comprehensive leaf model of Δ; and (5) test the predictive capabilities of three models: the comprehensive Farquhar *et al.* (1982) model of Δ (Δ_{comp}), a recently suggested amendment to Δ_{comp} ($\Delta_{revised}$; Wingate *et al.* 2007) and the simplified form of the comprehensive model (Δ_{simple}). We used a combined TDL-infrared gas analyser (IRGA) system to obtain high-frequency field measurements of leaf gas exchange synchronized with online isotopic measurements, similar to those used in previous greenhouse studies (Barbour *et al.* 2007a). Previous work has demonstrated substantial diurnal variation in leaf discrimination in diverse field settings including tropical forest (Harwood *et al.* 1998) and mesic conifer forest (Wingate *et al.* 2007). We report ~20 Δ measurements per hour over diurnal periods during both dry and wet seasons from a semi-arid woodland.

METHODS

The field site was located on Mesita Del Buey in Los Alamos, New Mexico, USA (35°50′N, 106°16′W; elevation 2140 m) in a piñon-juniper woodland (*Pinus edulis* Engelm. and *Juniperus monosperma* Engelm. Sarg., respectively) dominated primarily by juniper and understorey grasses and forbs (Breshears 2008; McDowell *et al.* 2008b). This semi-arid region typically has a bimodal precipitation regime, with substantial winter snowfall (October–April), followed by a dry period (May–June) and monsoonal precipitation from July through early September (Breshears 2008). Precipitation at our site in 2006 totaled 119 mm in winter and 224 mm in summer. Soils on the site are Typic Haplustalfs and Typic Ustochrepts (Davenport, Wilcox & Breshears 1996).

Leaf gas exchange measurements

We measured diurnal (0600–1900 h) leaf gas exchange from the bottom third of the canopy on two juniper trees on 12 June 2006, two different juniper trees on 11 July 2006 and a single juniper on 14 August 2006. We coupled a TDL (TGA100A; Campbell Scientific Inc., Logan, UT, USA) to a portable photosynthesis system (Li-Cor 6400; Li-Cor Biosciences, Lincoln, NE, USA) fitted with a conifer chamber (Li-Cor 6400-05) to quantify the concentration of CO_2 and its isotopologues $^{13}C^{16}O_2$ and $^{12}C^{16}O_2$ in gas entering and exiting the leaf chamber, herein referred to as the reference and sample gas streams (i.e. Barbour *et al.* 2007a). We supplied atmospheric air via a 50 L buffer volume to the Li-Cor 6400, which recorded the CO_2 and water vapour concentration of the reference and sample gas every 10 s. These same gas streams were dried to a constant low humidity and plumbed directly into the TDL using ultra-low porosity tubing (Synflex type 1300 $^1/_4$ in. diameter; Saint Gobain Performance Plastics, Northboro, MA, USA) wherein the TDL measured the CO_2 isotopologues $^{13}C^{16}O^{16}O$ and $^{12}C^{16}O^{16}O$ at a rate of 500 Hz. These 500 Hz data were then averaged down to 10 Hz, and all means were calculated from the 10 Hz data. Our 3 min TDL measurement cycle consisted of two reference tanks and the reference and sample gas streams, each measured for 45 s, from which we calculated means of isotopologue concentrations over the last 15 s of each inlet cycle. We combined these TDL data with IRGA-generated data after incorporating the 33 s lag between the two instruments.

We used a Li-Cor conifer chamber to maximize leaf area and allow natural light interception on the scalelike juniper foliage, regulating the chamber flow rate between 250 and 500 μmol s^{-1} to maintain a sufficient CO_2 drawdown and control chamber humidity. We attempted to maintain CO_2 drawdown $\geq$40 μmol CO_2 mol^{-1} air within the leaf chamber. Under moderate conditions, chamber temperature was unregulated, but under conditions of high ambient

air temperature (>35 °C) and solar radiation, the IRGA block temperature control was engaged to control leaf temperature below 35 °C, as measured by energy balance. On 12 June, we collected data from six leaf areas diurnally and from two leaf areas at night. On 11 July, we collected data from five leaf areas diurnally and two leaf areas during dark measurements. In both June and July, each leaf area was measured for 30 min to an hour and leaves were typically measured more than once each day. Finally, on 14 August, we collected all data from one leaf area diurnally during a 7 h period, and one leaf area during dark measurements. The isotopic signature of nocturnal respiration ($\delta^{13}C_{resp}$) was measured immediately following daylight measurements and beginning when ambient photosynthetic photon flux density (PPFD) fell below 30 μmol photons m^{-2} s^{-1} and foliage exhibited net CO_2 efflux. To achieve a true dark measurement, we applied a heavy shade cloth over the leaf chamber to reduce PPFD to zero and waited for stable chamber conditions (e.g. leaf temperature and respiration rate), which occurred within 5 min after the shade cloth was applied. We also determined the carboxylation capacity of these juniper trees on 22 June and 23 July 2007 using assimilation (A) responses to changes in substomatal CO_2 concentration (A/p_i). We collected these data using a Li-Cor 6400 fitted with a chamber light source (Li-Cor 6400-02B). We measured pre-dawn and midday xylem water potential (ψ_w) on 5 to 10 nearby juniper trees on each measurement day using a Scholander-type pressure bomb (PMS Instruments Co., Corvallis, OR, USA; McDowell *et al.* 2008b).

The working standard (WS) calibration tanks used during our diurnal measurements were calibrated against World Meteorological Organization (WMO)-certified standard tanks (541.67 μmol CO_2 mol^{-1} air, $\delta^{13}C = -16.16‰$ and 350.34 μmol CO_2 mol^{-1} air, $\delta^{13}C = -8.39‰$) within 24 h of each measurement campaign. The intertank calibration between WMO and WS tanks typically required 2 h to complete. Molar mixing ratios of $^{12}CO_2$:$^{13}CO_2$ in the WS tanks used in the June campaign were 354.04 ± 0.27:3.82 ± 0.003 μmol CO_2 mol^{-1} air (mean ± standard error; $n = 11$ inter-tank calibrations) and 563.85 ± 0.27:6.09 ± 0.003 μmol CO_2 mol^{-1} air ($n = 11$). Molar mixing ratios of $^{12}CO_2$:$^{13}CO_2$ in the WS tanks used in the July and August campaigns were 340.46 ± 0.29:3.67 ± 0.003 μmol CO_2 mol^{-1} air ($n = 10$) and 518.71 ± 0.08:5.60 ± 0.001 μmol CO_2 mol^{-1} air ($n = 6$). The WMO-certified tanks were filled and $\delta^{13}C$ calibrated at the Stable Isotope Lab (SIL) of the Institute for Arctic and Alpine Research, a cooperating agency of the Climate Monitoring division of the National Oceanic and Atmospheric Administration's Earth Research Laboratory. Measurement variation in the $\delta^{13}C$ of a known tank in the TDL measurement mode we used exhibited an SD of 0.06‰ across an hour and 0.20‰ across the day. To account for diurnal instrument drift, the TDL measured the high and low WS tanks during each 3 min cycle, and we calculated the deviation between the measured values and the known values to determine a gain and offset for each isotopologue in each tank being measured (Bowling *et al.* 2003). These gain and offset values were then applied to all data. The TDL measures the absolute concentration of each isotopologue, so the range of $^{12}CO_2$ and $^{13}CO_2$ in each WS tank should span the measurement range. During the three measurement days, our measurements occasionally exceeded the lower end of the total [CO_2] in our WS tanks (maximum deviation: 45.7 μmol mol^{-1}). To test that the calibration was valid below the lower tank, we used a WMO traceable standard tank (total [CO_2] = 142.86 μmol mol^{-1}, $\delta^{13}C = -7.96‰$) and an additional unknown tank that had a target total [CO_2] of 250 μmol mol^{-1}. We measured these two tanks and two WS tanks (344.88 μmol mol^{-1}, –8.16‰ and 548.16 μmol mol^{-1}, –16.42‰) in series. We calculated the total [CO_2] and isotope ratio of the unknown tank by calculating the gain and offset values in two ways: (1) using the span between the 142.86 μmol mol^{-1} tank and the 344.86 μmol mol^{-1} tank and (2) using the span between the 344.86 μmol mol^{-1} tank and the 548.16 μmol mol^{-1} tank measurements. The unknown tank was calculated to have a total [CO_2] of 247.44 μmol mol^{-1} and a $\delta^{13}C$ of –20.45‰ using the lower calibration span (#1), and a total [CO_2] of 247.43 μmol mol^{-1} and a $\delta^{13}C$ of –20.45‰ using the higher calibration span (#2), a net difference of 0.01 μmol mol^{-1} and 0.00‰. We also determined the [CO_2] and $\delta^{13}C$ of the 142.86 μmol mol^{-1} WMO tank using gain and offset values calculated using the higher calibration span (#2). The result was a total [CO_2] of 142.66 μmol mol^{-1} and a $\delta^{13}C$ of –7.88‰, a net difference of 0.20 μmol mol^{-1} and 0.08‰ from SIL-certified values. Based on this assessment, we conclude our TDL has a linear response that extends beyond the lowest CO_2 range we measured in this study.

The IRGA was calibrated the morning of each measurement day, and the reference and sample gas analysers of the IRGA were frequently matched to the same gas stream, while disconnected from the TDL inlet tubes. After reconnecting the TDL inlet tubes with the IRGA, the system was leak tested by gently blowing around the chamber, all connections and the pressure-equilibrating vent tube located on the sample line to the TDL. The TDL was also used to measure the reference and sample gas streams with an empty leaf chamber, and differences were lower than instrument precision (data not shown).

Δ and $\delta^{13}C_{resp}$ calculations

We calculated Δ_{obs} in the chamber following Evans *et al.* (1986):

$$\Delta_{obs} = \frac{\xi(\delta_o - \delta_e)}{1 + \delta_o - \xi(\delta_o - \delta_e)} \quad (1)$$

where $\xi = c_e/(c_e - c_o)$ is the ratio of the reference CO_2 concentration entering the chamber (c_e) relative to the sample CO_2 concentration outgoing from the chamber (c_o), and δ_e and δ_o are the $\delta^{13}C$ of the reference and sample gas, respectively. All variables incorporated in Δ_{obs} and $\delta^{13}C_{resp}$ (below) are derived from TDL measurements of [$^{12}CO_2$] and [$^{13}CO_2$], removing interinstrument variability. Mixing ratios of total [CO_2] were calculated following Barbour *et al.*

(2007a). Because the TDL measures the concentration of each isotopologue, δ_o and δ_e are calculated from the ratio of the molar abundance of each isotopologue and then presented in ratio to the Vienna Pee Dee belemnite (VPDB) standard, that is, $\delta = R_s/R_{VPDB} - 1$, where δ represents either δ_o or δ_e, and R_s and R_{VPDB} represent the carbon isotope ratio of the sample and VPDB standard, respectively. We determined $\delta^{13}C_{resp}$ following Barbour *et al.* (2007a):

$$\delta^{13}C_{resp} = \frac{\delta_o - \delta_e(1-p)}{p} \quad (2)$$

where p equals $(c_o - c_e)/c_o$. We estimated the $\delta^{13}C$ of assimilated sugars ($\delta^{13}C_s$) based on Farquhar *et al.* (1989), where $\delta^{13}C_s = (\delta_e - \Delta_{obs})/(\Delta_{obs} + 1)$. All other reported gas exchange values are calculated by the Li-6400 software following the methods of Farquhar, Caemmerer & Berry (1980), after correcting for leaf area. We determined the projected leaf area using a calibrated leaf area metre (Li-3100; Li-Cor Biosciences), and all gas exchange calculations are reported on a projected leaf area basis.

Model parameterization

We incorporated our data into the comprehensive model of leaf Δ (Farquhar *et al.* 1982; Farquhar & Richards 1984):

$$\Delta_{comp} = a_b\frac{p_a - p_s}{p_a} + a\frac{p_s - p_i}{p_a} + (b_s + a_w)\frac{p_i - p_c}{p_a} + b\frac{p_c}{p_a} - \frac{\frac{eR_d}{k} + f\Gamma^*}{p_a} \quad (3)$$

where a_b, a, a_w, b_s and b are the fractionation factors associated with CO_2 diffusion through the leaf boundary layer (2.9‰), stomata (4.4‰), water (0.7‰), fractionation attributed with CO_2 entering solution (1.1‰) and the net fractionation attributed to phosphoenolpyruvate carboxylase and ribulose-1,5-bisphosphate carboxylase/oxygenase activity (estimated at 29‰; Roeske & O'Leary 1984), respectively. The variables p_a, p_s, p_i and p_c represent the partial pressure (Pa) of CO_2 in the atmosphere surrounding the leaf, at the leaf surface, in the intercellular spaces and at the sites of carboxylation, respectively. The variables Γ^*, R_d, k, f and e represent the CO_2 compensation point (Pa) in the absence of day respiration, day respiration rate (μmol m^{-2} s^{-1}), carboxylation efficiency (μmol m^{-2} s^{-1} Pa^{-1}), and fractionations associated with photorespiration and day respiration (‰; see Table 1 for values), respectively. We calculated p_a, p_s and p_i by incorporating mole fraction measurements of $[CO_2]$ with atmospheric pressure in Los Alamos (mean = 79 kPa), and estimated p_c following Farquhar & Sharkey (1982):

$$p_c = p_i - A/g_i \quad (4)$$

where g_i is internal conductance to CO_2 (μmol m^{-2} s^{-1} Pa^{-1}). We chose a moderate g_i of 1.5 μmol m^{-2} s^{-1} Pa^{-1} based on the range of g_i values observed over the study period. Prevailing theory suggests Γ^* is highly conserved among C_3 species, and previous work has demonstrated a strong temperature dependence of the CO_2 photocompensation point (Jordan & Ogren 1984; Brooks & Farquhar 1985), on which we based our calculations of diurnal Γ^*. Our Γ^* calculations accounted for the reduced atmospheric pressure in Los Alamos, and we confirmed our estimates of Γ^* with those calculated using the Sharkey *et al.* (2007) A/p_i estimating utility (Table 1). Strictly, k, the carboxylation efficiency, is A/p_c; we used the initial slope of A/p_i response curves ($n = 10$) as a surrogate estimate and confirmed these slope-based results with calculations presented in Ku & Edwards (1977) and Wingate *et al.* (2007) (Table 1). Much work has demonstrated an inhibitory effect of light on respiration rate, even at an irradiance as low as 12 μmol m^{-2} s^{-1} (Atkin *et al.* 2000; Tcherkez *et al.* 2005, 2008). To facilitate estimation of R_d, we measured nocturnal respiration rate (PPFD = 0) on all 3 d for approximately 120 min after cessation of daytime measurements (see Results) and used these data to calculate an estimated R_d value for each day, where $R_d = 0.5R$ (Tcherkez *et al.* 2005) and R equals steady-state respiration rate 30–120 min post-illumination (Table 1). We parameterized the decarboxylation component of Δ_{comp} using constant f (8‰) (Rooney 1988; Tcherkez 2006) and e (–6‰) (Ghashghaie *et al.* 2003) values. Parameterizing e based on $\delta^{13}C_{resp}$ (typically estimated at –6‰) may be problematic because of shifts in respiratory biochemistry under illuminated conditions (Tcherkez *et al.* 2008). We assessed the magnitude of uncertainty introduced at high and low A when varying e by comparing $(R_d/A) \times (p_c/p_a)$ multiplied by values of $e = -6$ and –1‰, and calculating the resulting variation in the Δ_{ef} term (see Eqn 11).

We also ran model simulations following the recent revisions to the comprehensive model (Eqn 3) put forward by Wingate *et al.* (2007):

$$\Delta_{revised} = a_b\frac{p_a - p_s}{p_a} + a\frac{p_s - p_i}{p_a} + (b_s + a_w)\frac{p_i - p_c}{p_a} + b\frac{p_c}{p_a} - \frac{\frac{(e+e^*)R_d}{k} + f\Gamma^*}{p_a} \quad (5)$$

Table 1. Parameters used in model simulations of observed discrimination using the comprehensive model (Δ_{comp}) and the revised model ($\Delta_{revised}$). The fractionation factors associated with day respiration, e, and photorespiration, f, were assumed based on literature values while all the other terms are derived from our data

	Parameters						$\Delta_{revised}$ only
Day	k	R_d	Γ^*	e	f	g_i	e^*
12 June	0.38	1.23	2.86–5.23	–6	8	1.5	–11.5 to –1.6
11 July	0.40	2.2	3.17–5.17	–6	8	1.5	–12.5 to –0.9
14 August	0.40	1.83	2.43–4.29	–6	8	1.5	–10.5 to 1.2

where e^* represents apparent fractionation for day respiration expressing the difference between the isotopic composition of the respiratory substrate and photosynthetic assimilates at a given time (Table 1). We calculated an e^* value for each three minute isotopic measurement using the following equation:

$$e^* = \delta^{13}p_a - \Delta_{simple} - \delta^{13}C_{mean} \quad (6)$$

where $\delta^{13}p_a$ is the carbon isotope ratio of atmospheric air in the leaf chamber, and $\delta^{13}C_{mean}$ equals the mean calculated from the $\delta^{13}C_{resp}$ measurements for each measurement date (see Results). In $\Delta_{revised}$, we used a constant e, f, R_d, g_i and k and a temperature-dependent Γ^* (Table 1). Lastly, we modelled Δ for comparison to Δ_{obs} using the most simplified form of the Farquhar *et al.* (1982) model (Δ_{simple}), which eliminates boundary layer, g_i and decarboxylation contributions to CO_2 flux and their associated fractionation factors:

$$\Delta_{simple} = a + (b - a)\cdot\frac{p_i}{p_a} \quad (7)$$

where $b = 27‰$ (Gessler *et al.* 2008). All modelling was performed in Microsoft Excel XP Professional.

Estimation of g_i and Δ_{ef}

We estimated g_i following the slope-based approach (g_{is}) in Evans *et al.* (1986):

$$g_{is} = (b - b_s - a_w)/r_i \quad (8)$$

where r_i is the internal resistance to CO_2 transfer estimated as the slope of predicted ^{13}C discrimination minus Δ_{obs} versus A/p_a. In this application, predicted discrimination (Δ_i) was determined using Eqn 3 calculated with infinite g_i, i.e. $p_i = p_c$. In this study, variation in A/p_a was the result of natural variation in the leaf environment. We calculated slopes for each time period where new leaf material was enclosed in the leaf chamber, and tested each slope using a simple linear regression. All negative slopes were rejected because negative slopes result in negative g_{is} estimates. All regression analyses were performed using JMP 5.0.1 (SAS Institute Inc., Cary, NC, USA). We used significant ($P \leq 0.10$) slope values to estimate g_{is} for each foliage measurement, and determined the viability of each g_{is} estimate by comparing them to A across the entire measurement period. If the g_{is} estimate was too low to facilitate observed A during any portion of the measurement period, we deemed that estimate to be erroneous. Finally, based on the theory developed by Evans *et al.* (1986) and Caemmerer & Evans (1991), we used the y-intercept of significant g_{is} plots to estimate Δ_{ef}.

We also estimated g_i using the point-based method (g_{ip}; Evans *et al.* 1986):

$$g_{ip} = \frac{(b - b_s - a_w)\,A/p_a}{(\Delta_{pred} - \Delta_{obs}) - \Delta_{ef}} \quad (9)$$

where Δ_{pred} represents a simplified predictive model of leaf Δ:

$$\Delta_{pred} = a_b\frac{p_a - p_s}{p_a} + a\frac{p_s - p_i}{p_a} + b\frac{p_i}{p_a} \quad (10)$$

and Δ_{ef} is calculated as:

$$\Delta_{ef} = \frac{\frac{eR_d}{k} + f\Gamma^*}{p_a} \quad (11)$$

where all factors are the same as described in Δ_{comp} (Eqn 3).

g_i sensitivity analysis

We assessed the sensitivity of Δ_{comp} to changes in g_i by holding all parameters listed in Table 1 constant and by varying the g_i value used to calculate p_c over each day. We used g_i values ranging from 0.5 to 2.5 μmol m^{-2} s^{-1} Pa^{-1}, and applied each value uniformly across each measurement day.

Statistical analysis

We estimated the error in Δ_{obs} and $\delta^{13}C_{resp}$ by implementing the parametric bootstrap (Davison & Hinkley 1997); we describe the procedure for Δ_{obs}, but $\delta^{13}C_{resp}$ can be substituted in the description. For each measurement cycle, we used the sample mean and SEs of the concentrations of $^{12}CO_2$ and $^{13}CO_2$ for the high WS tank, low WS tank, reference gas and sample gas to define eight normal distributions. We drew eight random deviates of [$^{12}CO_2$] and [$^{13}CO_2$] from these distributions, calculated a bootstrap replicate of Δ_{obs}, and repeated this 10 000 times to provide a bootstrap sampling distribution of Δ_{obs}. This insured that the variance measured with each isotopologue was propagated into each calculation of c_e, c_o, ξ, δ_e and δ_o and, therefore, into Δ_{obs} and $\delta^{13}C_{resp}$. The SE of the bootstrap replicates provides an estimate of the SE of Δ_{obs}. We observed that the bootstrap sampling distributions of Δ_{obs} were roughly normal, so the estimated SE characterizes the variation in Δ_{obs}. All bootstrap analyses were performed in R (R Core Development Team 2008) .

For both g_{is} and g_{ip}, the g_i estimate is a reciprocal transformation of a normally distributed random variable. While the SEs describe the normal distributions well, they are not easily interpretable for the skewed distributions associated with g_{is} and g_{ip}. g_{is} is the reciprocal of r_i, estimated using the normally distributed regression slope (Table 2). For the slope-based g_i, we calculated r_i and $r_i \pm 1$ SE, and transformed these three values to the g_i scale (Eqn 8) to generate g_i and an estimate of its error. Similarly, for the point-based g_i, we calculated the roughly normally distributed bootstrap mean $\Delta_{obs} \pm 1$ SE and transformed these to the g_i scale

Campaign	Time (h)	Slope	SE	*P*	Δ_{ef}	SE	*P*	r^2
12 June	0700	22.05	11.13	0.06	–2.19	1.74	0.22	0.18
	1300	108.63	46.77	0.05	–10.56	5.35	0.08	0.40
11 July	0900	54.81	22.07	0.05	–12.03	6.4	0.11	0.51
	1200	20.4	10.49	0.09	–3.83	2.29	0.14	0.35
	1300	27.58	10.55	0.03	–3.58	2.13	0.14	0.49
	1400	27.32	7.72	0.02	–4.91	2.03	0.06	0.71
	1500	21.44	7.65	0.01	–3.53	1.79	0.07	0.34
	1600	29.31	12.35	0.05	–3.12	2.54	0.25	0.41
14 August	0600	757.31	312.02	0.07	–21.31	5.87	0.02	0.60
	0700	87.24	23.82	0.008	–1.28	1.52	0.42	0.66
	0800*	22.81	15.53	0.18	–0.41	2.94	0.89	0.21
	0900	20.21	4.39	0.0002	0.15	0.63	0.8	0.54
	1000*	15.23	8.47	0.11	1.39	1.52	0.39	0.29
	1100	43.04	7.68	0.0005	–3.33	0.89	0.006	0.80
	1200*	13.17	8.86	0.18	–2.11	2.77	0.47	0.22
	1300	12.69	3.83	0.01	–1.54	1.19	0.23	0.58

Table 2. Slope and intercept statistics from linear regressions used to calculate g_{is} and estimate Δ_{ef}. Cut-off values for the test of slope significance within each regression was $P \leq 0.10$, but three marginal slopes are also represented (*). Most intercepts were not significantly different from zero, but significant intercepts ($P \leq 0.10$) deviated substantially from zero

(Eqn 9). For these data, 1 SE on the r_i or Δ_{obs} scale is asymmetric on the g_i scale with the upper SE being roughly twice the lower SE.

To assess model performance, we first used least squares regression analysis of predicted and observed values but found that the residual analysis of data in all months and models exhibited a non-random distribution. Additionally, both the slope and intercept terms were significantly different from one and zero, respectively, and substantially different from one another, making model comparisons difficult to evaluate. We then modified the computation of the residuals so that all models conformed to a slope of one and an intercept of zero (i.e. residuals = model prediction – observed data), and calculated the SD of the residuals. These SD values represented the square root of the sum of the variance and squared model bias, or the root mean square error (RMSE), for each month and model, and facilitated a direct comparison of the predictive performance between models within each month.

RESULTS

Diurnal Δ_{obs}

Juniper Δ_{obs} averaged (mean ± SE) 16.3 ± 0.2‰ in June, 17.2 ± 0.2‰ in July and 19.0 ± 0.5‰ in August ($P \leq 0.0002$ between each). Leaf Δ_{obs} tended to be highest in the early morning in all three months, followed by midmorning variability and a decline through much of the afternoon (Fig. 1). The seasonal Δ_{obs} trend tracked the transition from low (June) to high (August) soil, leaf and atmospheric water content (Table 3, Fig. 2d–f). Similarly, the diurnal trend towards lower Δ_{obs} in the afternoon reflects the transition from relatively high morning leaf ψ_w to lower midday ψ_w (Table 3). On July and August measurement days, the variation in leaf Δ_{obs} reflects the stability of the light environment, with a relatively stable PPFD in July concurrent with a stable Δ_{obs} and a heterogeneous light environment in August resulting in fluctuating Δ_{obs} (Fig. 2). On 14 August, we lack reliable isotopic data after 1300 h because of low ambient light (PPFD < 100 μmol m^{-2} s^{-1}), preventing A rates high enough to sustain reliable isotopic measurements. We found a weak but significant correlation between leaf vapour pressure deficit (VPD) and Δ_{obs} ($r^2 = 0.20$,

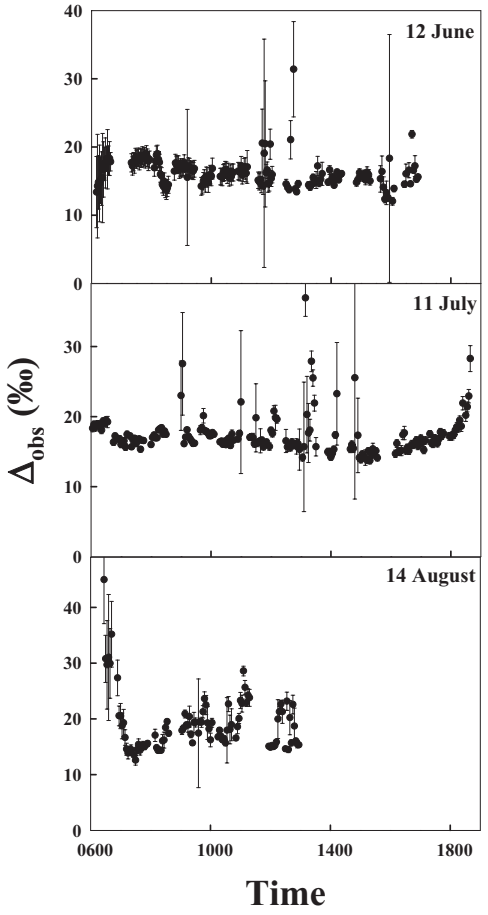

Figure 1. Diurnal variation in carbon isotope discrimination (●; Δ_{obs}) on 12 June, 11 July and 14 August. Error bars represent 1 SE. Note the change of *y*-axis scaling in panels.

Table 3. Mean xylem water potential with SE on all three measurement days. Midday values from McDowell *et al.* (2008b)

	Pre-dawn ψ_w (MPa)	SE	Midday ψ_w (MPa)	SE
June	–2.47	0.14	–2.93	0.85
July	–0.67	0.03	–1.99	0.03
August	–0.58	0.04	–1.58	0.44

$P < 0.0001$; $F = 110.22$; Fig. 3), PPFD and Δ_{obs} ($r^2 = 0.20$, $P < 0.0001$; $F = 114.11$), and A and Δ_{obs} ($r^2 = 0.11$, $P < 0.0001$; $F = 54.97$; Fig. 3) using data pooled across all 3 d. Excluding the seven very high Δ_{obs} values in the early August morning, there was a significant relationship between stomatal conductance (g_s) and Δ_{obs} ($r^2 = 0.03$, $P < 0.0001$; $F = 16.60$; Fig. 3).

Nocturnal $\delta^{13}C_{resp}$

The isotopic composition of nocturnal respiration was similar in June (mean = –22.6 ± 0.2‰) and July (mean = –22.7 ± 0.2‰; $P = 0.70$) (Fig. 4), while respiration rates were dissimilar (2.6 ± 0.04 and 4.8 ± 0.1 μmol m^{-2} s^{-1}, respectively; $P < 0.0001$). In August, mean $\delta^{13}C_{resp}$ was more depleted (mean = –23.5 ± 0.1‰) than values measured in June ($P < 0.0001$) and July ($P < 0.0001$), while respiration rate (mean = 3.7 ± 0.004 μmol m^{-2} s^{-1}) was higher than that observed in June ($P < 0.0001$) and lower than that observed in July ($P < 0.0001$). These $\delta^{13}C_{resp}$ values were enriched compared with estimates of the composition of recently assimilated sugars, which were –24.66 ± 0.20‰ in June, –25.19 ± 0.17‰ in July and –25.97 ± 0.30‰ in August. The step change in $\delta^{13}C_{resp}$ observed approximately 50 min post-illumination in June and July was due to cessation of measurement on one group of foliage and the movement to new foliage.

Temporal variation in g_i and Δ_{ef}

We tested 32 slopes and found that 17 were significant across the 3 d. These produced 14 viable g_{is} and Δ_{ef} estimates based on comparisons to A, including two in June, six in July and six in August (Fig. 5; Table 2). We also found three slopes in the August morning, which failed our criteria for having a significant slope ($P \leq 0.1$), but whose estimates of g_{is} fit the observed trend and are included in Fig. 5 (Table 2). Other g_{is} estimates failed to support observed A or displayed negative slope relationships between Δ_i–Δ_{obs} and A/p_a, and were excluded from the analysis. Estimates of g_{ip} produced non-viable values when Δ_{obs} was larger than Δ_{pred} in bootstrap resamples, resulting in negative g_{ip} estimates. These 98 negative values, representing 22% of all g_{ip} estimates, were excluded from the analysis.

Internal conductance calculated from slope-based measurements ranged from 0.04 to 2.14 μmol m^{-2} s^{-1} Pa^{-1} (mean ± SE = 1.06 ± 0.17 μmol m^{-2} s^{-1} Pa^{-1}) across the 3 d. The 14 August g_{is} measurements were obtained from one leaf area across the morning and early afternoon, and demonstrated an increase in g_{is} from 0.04 to 2.14 μmol m^{-2} s^{-1} Pa^{-1} (Fig. 5c). We observed a lower range of variability in July g_{is}, with afternoon values ranging between 0.92 and 1.3 μmol m^{-2} s^{-1} Pa^{-1}. We did not find a significant relationship between leaf temperature (T_l) and g_{is} ($r^2 = 0.003$, $P = 0.87$; $F = 0.028$). Estimates of g_{ip} ranged between 0.05 and 8.53 μmol m^{-2} s^{-1} Pa^{-1} (mean ± SE = 1.89 ± 0.07 μmol m^{-2} s^{-1} Pa^{-1}) across the three measurement days (Fig. 5). Sensitivity analysis demonstrated a significant increase ($P < 0.0001$) in g_{ip} estimates when varying $e = –6$‰ and $f = 8$‰ (mean ± SE = 1.60 ± 0.04 μmol m^{-2} s^{-1} Pa^{-1}) to $e = –1$‰ and $f = 11$‰ (3.31 ± 0.14 μmol m^{-2} s^{-1} Pa^{-1}). There was a small but significant relationship between g_{ip} and T_l ($r^2 = 0.03$, $P = 0.0003$; $F = 13.168$).

Δ_{ef} also exhibited diurnal variation, ranging between –21.3 and +1.34‰. In August, we observed a low Δ_{ef} value of –21.3‰ in the early morning, later morning values that were not significantly different from zero ($P \leq 0.10$), and afternoon values near –2.5‰ (Table 2). The morning value in July was not significantly different from zero, whereas the afternoon Δ_{ef} values were between –4.9 and –3.5‰. Our single significant Δ_{ef} value in June was –10.56 ± 5.3‰. The non-zero values of Δ_{ef} occur at early morning, midday or late afternoon, when fluxes are small and errors are likely to be greatest (Table 2).

Δ_{obs} and p_i/p_a

First-order linear relationships between Δ_{obs} and p_i/p_a were significant in June ($r^2 = 0.25$, $P < 0.0001$; $F = 58.31$; Fig. 6a), July ($r^2 = 0.51$, $P < 0.0001$; $F = 182.61$) and August ($r^2 = 0.72$, $P < 0.0001$; $F = 248.99$); however, second-order polynomials described the relationships with greater predictive power in July ($r^2 = 0.64$, $P < 0.0001$; $F = 151.90$) and August ($r^2 = 0.88$, $P < 0.0001$; $F = 334.27$; Fig. 6b,c). The curvilinear relationship between Δ_{obs} and p_i/p_a was most pronounced in the p_i/p_a range between 0.75 and 0.85.

g_i sensitivity analysis

Incorporation of variable g_i into Δ_{comp} over diurnal periods produced variation in predictions of Δ_{comp}. Sensitivity analysis demonstrated using low g_i (0.5 μmol m^{-2} s^{-1} Pa^{-1}) in Δ_{comp} resulted in a mean 6.9‰ underestimate of Δ_{obs}, while relatively high g_i (2.5 μmol m^{-2} s^{-1} Pa^{-1}) resulted in a 0.70‰ overestimate of Δ_{obs} (Table 4). Pairwise comparisons of the residuals (Δ_{obs}–Δ_{comp}) resulting from Δ_{comp} predictions incorporating a g_i value of 0.5 μmol m^{-2} s^{-1} Pa^{-1} were significantly different from the residuals produced when using g_i values of 1.0, 1.5, 2.0 and 2.5 μmol m^{-2} s^{-1} Pa^{-1} in Δ_{comp} [$P \leq 0.05$; Tukey's Honestly Significant Differences (HSD)] within and across all 3 d. Similarly, all other g_i inputs into Δ_{comp} (1.0, 1.5, 2.0 and 2.5 μmol m^{-2} s^{-1} Pa^{-1}) produced significantly different residuals from one another within each day and across all 3 d (Table 4). The RMSE, a measure of the variance and squared bias associated with the residuals, largely followed the trend observed in the pairwise residual

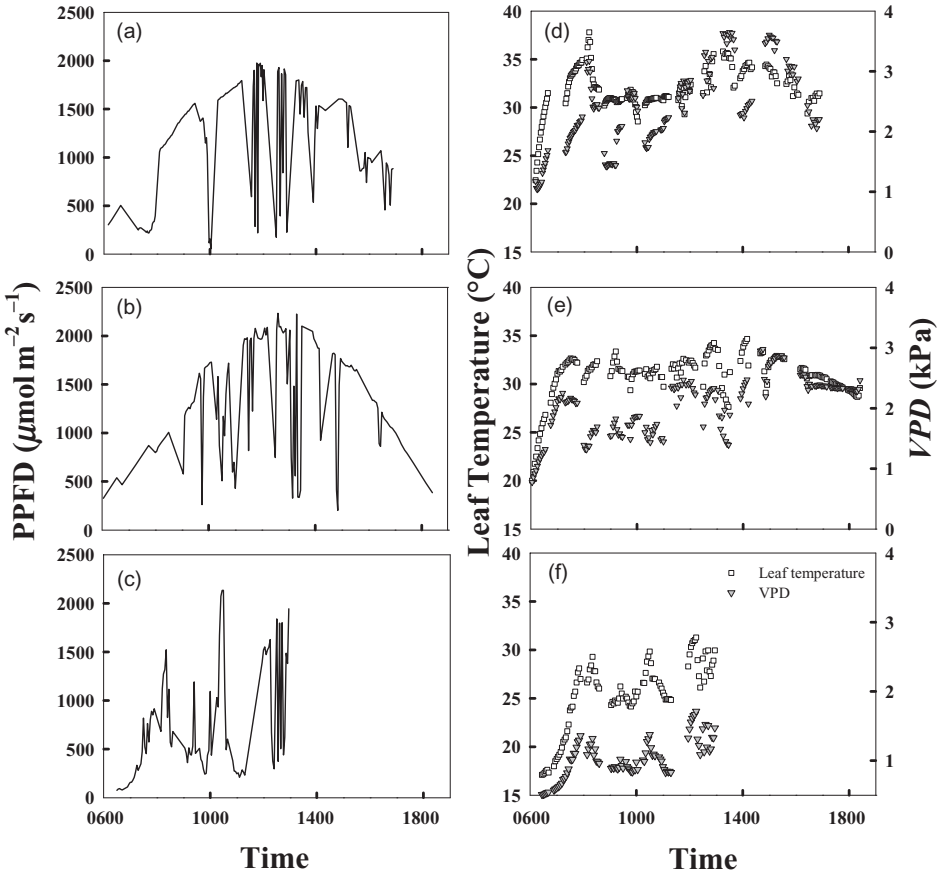

Figure 2. Environmental parameters on each measurement day. Panels a–c depict incident photosynthetic photon flux density (PPFD) trends across each measurement day. Panels d–f show leaf temperature, as measured by energy balance (□) and vapour pressure deficit (VPD; ▽) across each measurement day.

comparisons and was lower when residual differences were smaller; this demonstrates the importance of an accurate estimate of g_i for model fit. Internal conductance values of 1.5 and 2.0 μmol m^{-2} s^{-1} Pa^{-1} produced the best predictions, as determined by the lowest pairwise residual differences and RMSE, when applied uniformly across each measurement day (Table 4).

Model predictions: Δ_{comp}, $\Delta_{revised}$ and Δ_{simple}

Model performance varied across the three measurement days (Fig. 7). Assessing the error between model predictions and Δ_{obs} in each month showed that Δ_{simple} had the lowest RMSE, 2.11‰, in June, Δ_{comp} had the lowest error in July (RMSE = 1.50‰), and $\Delta_{revised}$ exhibited the lowest error in August (RMSE = 3.15‰; Table 5). Substituting b = 25‰ into Δ_{simple} reduced model prediction bias (mean = 0.31 ± 0.12‰) but resulted in higher RMSE (mean = 2.65‰ versus 2.42‰ for b = 27‰) on all 3 d compared with using b = 27‰. The estimated model prediction bias between Δ_{comp}, $\Delta_{revised}$ and Δ_{simple} and observed discrimination across all three dates was (mean ± SE) –0.62 ± 0.18‰, –0.28 ± 0.19‰ and 1.63 ± 0.18‰, respectively. However, error assessment revealed that the apparent close simulations suggested by the small model prediction bias between modelled and observed values masked substantial variance in all models' predictions of Δ_{obs} (Table 5). At high A, defined here as >4.0 μmol m^{-2} s^{-1}, uncertainty introduced into Δ_{ef} by utilizing e = –6‰ versus –1‰ was equal to 2.21 ± 0.01‰, while at low A, defined here as <2.0 μmol m^{-2} s^{-1}, the same uncertainty increased to 9.40 ± 1.51‰ (Table 6).

DISCUSSION

The objectives of this study were to (1) examine the temporal variation in Δ, $\delta^{13}C_{resp}$, g_i and Δ_{ef} under ambient field conditions; (2) test the hypothesis that g_i varies across the day; (3) test the hypothesis that Δ varies linearly in response to shifts in p_i/p_a under field conditions; (4) test the influence of g_i in a comprehensive leaf model of Δ; and (5) test the predictive capabilities of three models: the comprehensive Farquhar *et al.* (1982) model of Δ (Δ_{comp}), a recently suggested amendment to Δ_{comp} ($\Delta_{revised}$; Wingate *et al.* 2007) and the simplified form of the comprehensive model (Δ_{simple}). We observed a large range of variation in Δ, g_i and Δ_{ef} over diurnal time periods and across the season. Seasonally, $\delta^{13}C_{resp}$ decreased as water availability increased. We found that g_i varied across the day in August and that g_i exerted

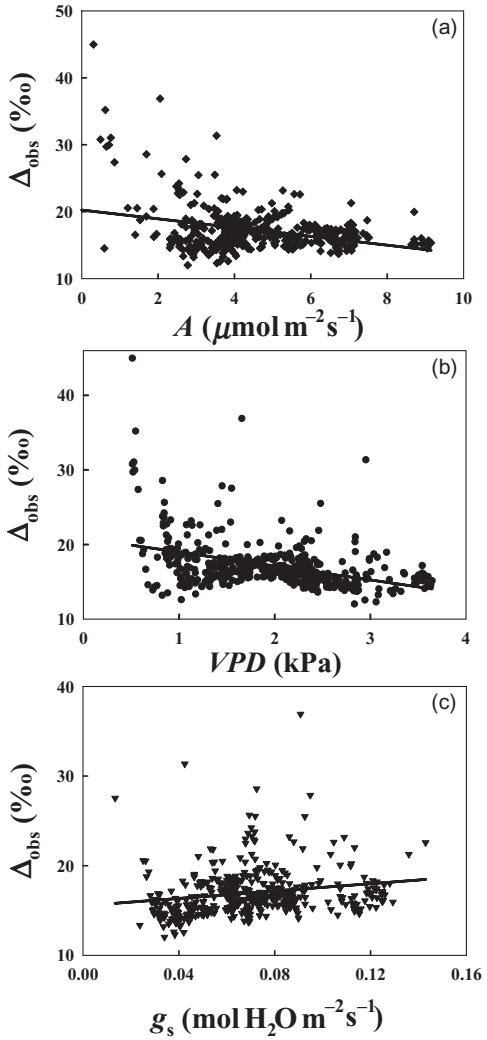

Figure 3. The relationship between observed discrimination (Δ_{obs}) and net photosynthetic rate (A; a), leaf-to-atmosphere vapour pressure deficit (VPD; b) and stomatal conductance (g_s; c). Δ_{obs} exhibited a significant correlation with pooled leaf A ($r^2 = 0.11$, $P < 0.0001$) and VPD ($r^2 = 0.20$, $P < 0.0001$). Excluding seven high August morning values, Δ_{obs} exhibited a significant relationship with g_s ($r^2 = 0.03$, $P < 0.0001$).

substantial influence on Δ predictions. We found Δ_{obs} varied in a linear fashion in response to p_i/p_a in June, but second-order expressions better described the relationship in July and August. Finally, we found all models reasonably predicted Δ_{obs}, but Δ_{simple} best predicted Δ_{obs} in June, Δ_{comp} best predicted Δ_{obs} in July, and $\Delta_{revised}$ best predicted Δ_{obs} in August.

Diurnal Δ_{obs} and nocturnal $\delta^{13}C_{resp}$

Diurnal Δ_{obs} in our juniper woodland varied between 12.0 and 27.4‰, which was similar in trend and magnitude to Δ observed in a tropical forest (Harwood *et al.* 1998) and in a mesic *Picea* stand (Wingate *et al.* 2007) (Fig. 1). Variation in Δ_{obs} was generally related to environmental drivers such as PPFD and VPD (Figs 1–3). An inverse relationship between VPD and Δ_{obs} was apparent diurnally and seasonally, although low leaf ψ_w and high air temperature likely contributed to low discrimination in June compared with July and August. In August, VPD was relatively low and cloudy conditions caused large variation in Δ_{obs}. Cumulatively, these sensitivities to VPD and PPFD were similar to those seen in modelled canopy Δ (Baldocchi & Bowling 2003; Chen & Chen 2007). We also observed several high, but transient, discrimination values in all 3 months including midday values of 31.4‰ in June and 36.9‰ in July, and observations ranging from 29.7 to 44.9‰ in the early morning in August. These Δ_{obs} values were associated with greater uncertainty, but were similar to values observed in *Piper* and *Picea* (Harwood *et al.* 1998; Wingate *et al.* 2007).

Nocturnal $\delta^{13}C_{resp}$ for the juniper trees in our study ranged from ~ –24 to –21‰, and was moderately enriched compared with most observations in the literature (Bowling *et al.* 2002; Hymus *et al.* 2005; Prater, Mortazavi & Chanton 2005). $\delta^{13}C_{resp}$ values were similar in June and July, and were more enriched in ^{13}C compared with the values in August (Fig. 4). The consistent 2–3‰ enrichment of $\delta^{13}C_{resp}$

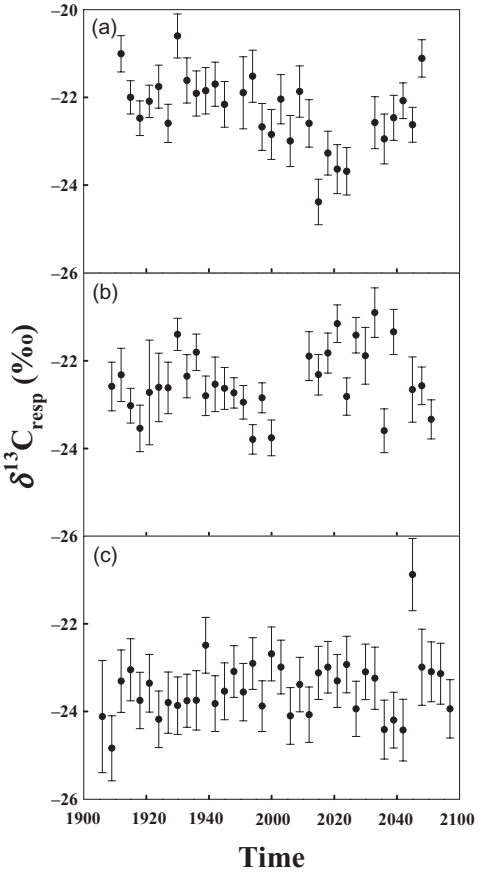

Figure 4. The ratio of $^{13}CO_2$ to $^{12}CO_2$ in post-illumination nocturnal respiration (●; $\delta^{13}C_{resp}$) on the evening of 12 June (a), 11 July (b) and 14 August (c). $\delta^{13}C_{resp}$ was similar in June and July ($P = 0.70$), but $\delta^{13}C_{resp}$ in August was more significantly more ^{13}C depleted than in June ($P < 0.0001$) and July ($P < 0.0001$). Error bars represent 1 SE.

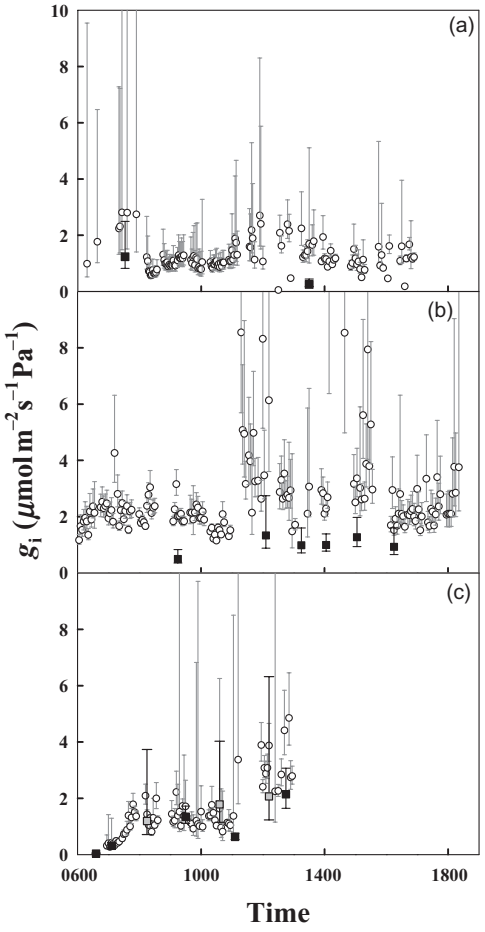

Figure 5. Diurnal variation in internal conductance of CO_2 estimated using sloped-based methods (■; g_{is}) and point-based methods (○; g_{ip}) on 12 June (a), 11 July (b) and 14 August (c). Internal conductance values derived from non-significant slopes ($P \geq 0.10$) on 14 August are also represented (□); all g_i estimates from 14 August were measured on one leaf area. Error bars represent 1 SE and are presented with grey (g_{ip}) and black (g_{is}) lines.

compared to estimates of recently assimilated carbohydrate is consistent with previous reports (Duranceau *et al.* 1999; Ghashghaie *et al.* 2001) and may reflect respiratory fractionation, possibly combined with diverse respiratory substrate utilization (Tcherkez *et al.* 2003). This $\delta^{13}C_{resp}$ pattern is consistent with the temporal transition period from drought in June through the onset of summer monsoon in July to the strong monsoon in August.

Temporal variation in g_i and Δ_{ef}

We observed a diurnal increase in g_i occurring in one leaf area across the August morning and early afternoon, and a range of variation in g_i across the 3 months (Fig. 5). The physiological drivers of this variation in g_i are unknown, but likely involved changes in protein activity facilitating the transfer of CO_2 across cell or chloroplast membranes (Flexas *et al.* 2006; Hanba *et al.* 2006; Uehlein *et al.* 2008). Previous work has demonstrated variability in g_i in response to environmental variables such as temperature (Bernacchi *et al.* 2002; Warren & Dreyer 2006; Yamori *et al.* 2006) and water availability (Warren *et al.* 2004; Grassi & Magnani 2005; Galmés, Medrano & Flexas 2007; Diaz-Espejo *et al.* 2007), both of which fluctuate in a field setting. We did not find a significant correlation between T_l and g_{is}, but we did find a significant relationship between T_l and g_{ip}. It is possible that variable irradiance over each measurement period may have confounded any temperature effect on g_{is}, but the higher temporal frequency of g_{ip} was closer to the frequency T_l was changing diurnally. Juniper displays anisohydric leaf hydraulic behaviour, and concurrent ψ_w measurements (Table 3) demonstrated a seasonal increase and diurnal decrease in xylem ψ_w. The seasonal ψ_w pattern paralleled our seasonal g_i measurements, suggesting a linkage between leaf water status and the g_i patterns we observed, but are confounded by the increase in both g_{is} and g_{ip} in the August morning when ψ_w was decreasing. Notably, there was a distinct decrease in g_{is} in the upward morning trend that coincides with extended cloud cover (mean

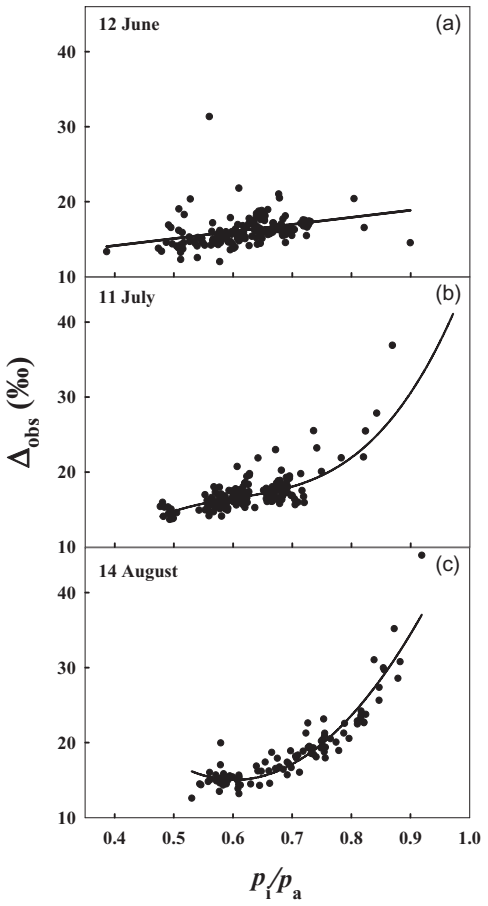

Figure 6. The relationship between observed discrimination (Δ_{obs}) and p_i/p_a. First-order linear relationships were observed in June (a; $r^2 = 0.25$, $P < 0.0001$), July (b; $r^2 = 0.51$, $P < 0.0001$) and August (c; $r^2 = 0.72$, $P < 0.0001$) although second-order polynomial relationships better described the data in July ($r^2 = 0.64$, $P < 0.0001$) and August ($r^2 = 0.88$, $P < 0.0001$).

Table 4. Results from a sensitivity analysis utilizing variable g_i values within Δ_{comp} and applied across each measurement day. $\Delta_{obs} - \Delta_{comp}$ represents the pairwise residual difference (‰) between observed discrimination (Δ_{obs}) and model predictions (Δ_{comp}). Δ_{comp} predictions using each of the g_i values produced residuals significantly different from one another within each day and across days. As determined by the lowest root mean square error (RMSE; ‰) and pairwise residual difference, g_i of 1.5 and 2.0 μmol m^{-2} s^{-1} Pa^{-1} performed best in predicting Δ_{obs}

	June	$n = 177$	July	$n = 176$	August	$n = 97$
g_i	Δ_{obs}–Δ_{comp}	RMSE	Δ_{obs}–Δ_{comp}	RMSE	Δ_{obs}–Δ_{comp}	RMSE
0.5	4.77	2.24	9.61	2.24	6.56	4.95
1.0	1.02	1.85	3.58	1.55	2.06	3.06
1.5	–0.22	1.77	1.57	1.51	0.55	2.66
2.0	–0.85	1.74	0.57	1.53	–0.20	2.54
2.5	–1.22	2.13	–0.04	1.56	–0.84	3.13

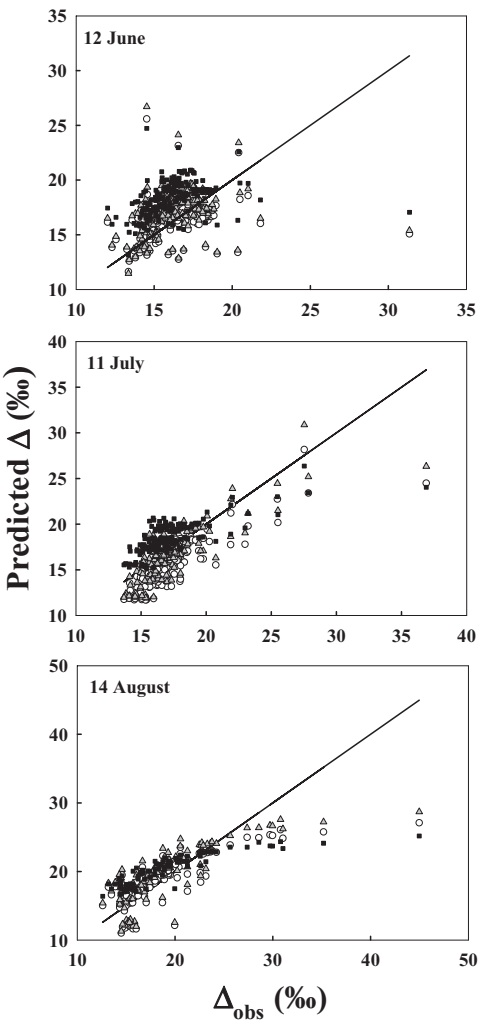

Figure 7. The relationship between observed discrimination (Δ_{obs}) and discrimination values predicted using $\Delta_{revised}$ (△), Δ_{comp} (○) and Δ_{simple} (■) relative to the 1:1 Δ_{obs} line (solid line). Note: axes are unequal among panels to enhance resolution. $\Delta_{revised}$ and Δ_{comp} utilized a $b = 29$‰, while Δ_{simple} was fit with a $b = 27$‰; other parameters are listed in Table 1. Δ_{simple} exhibited the lowest overall error in predicting Δ_{obs} in June, Δ_{comp} exhibited the lowest error in July, and $\Delta_{revised}$ exhibited the lowest error in August.

PPFD = 266 ± 46 μmol m^{-2} s^{-1}). We speculate that the large and prolonged drop in incident light played a regulatory role in the lower g_i, similar to observations of other environmental regulators of g_i in controlled studies (Delfine *et al.* 1999; Bernacchi *et al.* 2002; Flexas *et al.* 2007). The July data exhibit modest variation in diurnal g_i, but may reflect natural variation among branches. Given that our measurements were collected under ambient environmental conditions, an accurate assessment of the factors driving the variation in g_i we observed is not possible and should be addressed in controlled studies.

The variation in g_{is} is potentially problematic for the slope-based method because it assumes that g_i is constant over the period the slope data are collected. While rapid variation in g_i has been demonstrated in response to [CO_2] (Flexas *et al.* 2007), the rate and magnitude of diurnal shifts in g_i under field conditions have not been previously reported. Our 30–45 min g_{is} measurement periods may have spanned too long and allowed time for g_i to change in response to the environment. However, aside from periods where Δ_{obs} was highly variable, such as the July midday period, g_{ip} values were generally stable around each g_{is} value and show that variation was low enough to provide valid g_{is} estimates. Slope-based estimates of g_i tended to be lower than g_{ip} in June and July, but both trended together in August (Fig. 5). g_{ip} is sensitive to the parameterization of *e* and *f*, and errors in estimating these values may have resulted in over- or underestimation of *g*.

Most of our g_i estimates agree with values reported in other woody species (Lloyd *et al.* 1992; De Lucia, Whitehead & Clearwater 2003; Warren *et al.* 2003; Ethier *et al.* 2006), but we also found low g_{is} estimates in the early morning and relatively high g_{ip} estimates when Δ_{obs} was highly variable. We found a low g_{is} estimate (0.03 μmol m^{-2} s^{-1} Pa^{-1}) in the August early morning transition period from respiration to net *A*, where net CO_2 drawdown was between 6 and 10 μmol mol^{-1}, uncertainty in Δ_{obs} was higher, and measurements may have been more strongly influenced by the isotopic signature of CO_2 evolved during concurrent day respiratory processes. Although low, model simulations demonstrated that the 0.03 μmol m^{-2} s^{-1} Pa^{-1} conductance estimate was high enough to allow observed *A* across the measurement period. Estimates from g_{ip} during this period

Table 5. Comparison of model performance in predicting Δ_{obs}. Means represent the difference between model predictions and Δ_{obs} (bias) and the root mean square error (RMSE). Δ_{simple} consistently overestimated Δ_{obs} but showed a lower error in predicting Δ_{obs} in June compared with Δ_{comp} and $\Delta_{revised}$. Δ_{comp} exhibited the lowest error in July, while $\Delta_{revised}$ exhibited a lower error and mean difference between predicted and observed values in August compared with Δ_{simple} and Δ_{comp}

	June bias ‰	$n = 177$ RMSE ‰	July bias ‰	$n = 176$ RMSE ‰	August bias ‰	$n = 97$ RMSE ‰
Δ_{simple}	2.23	2.11	1.32	1.80	1.12	3.48
Δ_{comp}	0.28	2.30	–1.58	1.50	–0.55	3.19
$\Delta_{revised}$	0.79	2.39	–0.68	1.61	0.34	3.15

show consistently negative estimates of g_i (data not shown). High and variable g_{ip} estimates ranged between 4 and 8 μmol m^{-2} s^{-1} Pa^{-1} during the midday period in July, driven by higher uncertainty in Δ_{obs} over this period.

Our measurements of Δ_{ef} suggest that fractionations attributed to decarboxylation activity may not be negligible at dawn and in the afternoon when rates of either respiration or photorespiration may be high (Table 2). Our early morning August measurement occurred during a time of low A/p_a and generated a very negative Δ_{ef} value. If respiration had not fully deactivated to its daytime rate, then it may have had an unusually large impact during that time period (Gillon & Griffiths 1997). By midmorning in July and August, A and g_s had reached a plateau, and Δ_{ef} was not significantly different from zero. However, in the June and July afternoons, high temperature and PPFD created conditions conducive to higher photorespiration rates that may have contributed to greater variation in the afternoon Δ_{ef} values. Further, compared with other C_3 species, juniper exhibits high R, from which we estimated R_d, and thus the respiratory component of Δ_{ef} would have a larger impact on net Δ than would be expected for other species. Carefully controlled studies partitioning different components of the net flux will be necessary to elucidate the contribution of each component.

Δ_{obs} and p_i/p_a

We observed significant first-order linear relationships between Δ and p_i/p_a in all months, but found that second-order models better described the curvilinear relationship between Δ and p_i/p_a in July and August (Fig. 6). We propose that the curvilinear relationship is related to the increasing dominance of respiration and associated isotopic signatures on leaf-exchanged CO_2 at high p_i/p_a values. Previous work and theory have demonstrated a linear relationship between Δ and p_i/p_a in C_3 plants (Farquhar *et al.* 1982b, 1989; Evans *et al.* 1986; Brugnoli *et al.* 1988), but unlike our study, these data were collected in controlled settings under steady-state conditions. In both July and August, the curvilinear trend between Δ and p_i/p_a was driven by high Δ values. These high Δ values correspond with conditions conducive to high respiratory and photorespiratory flux, notably the early morning and midday periods, and may reflect the isotopic signature of a highly enriched substrate.

Table 6. Results from a sensitivity analysis assessing the variation in Δ_{ef}, the decarboxylation term in Δ_{comp}, when parameterized with $e = -6$‰ and $e = -1$‰. The uncertainty introduced into the decarboxylation term at low to high net photosynthetic rate (A) when varying e from –6 to –1‰ is represented in Δ_{ef} uncertainty (‰). This demonstrates that Δ_{ef} is very sensitive to variation in e at low A; in this study, <4% of all measurements were at $A < 2.0$ μmol m^{-2} s^{-1}

A (μmol m^{-2} s^{-1})	Δ_{ef} uncertainty (‰)	SE
<2.00	9.40	1.51
2.00–3.99	2.64	0.04
4.00–9.15	2.21	0.01

g_i sensitivity analysis

Incorporating variable internal CO_2 conductance into Δ_{comp} demonstrated that g_i exerted substantial influence on predictions of diurnal discrimination. Average-observed g_i was near 1.5 μmol m^{-2} s^{-1} Pa^{-1}, and our sensitivity analysis showed that relatively low (0.5 μmol m^{-2} s^{-1} Pa^{-1}) and high (2.5 μmol m^{-2} s^{-1} Pa^{-1}) values resulted in large deviations between model predictions and Δ_{obs} (Table 4). However, we have shown that g_i can vary in a leaf over several hours, and it is likely that incorporating this diurnal variability into leaf and ecosystem models would improve discrimination predictions (McDowell *et al.* 2008a). Future studies should focus on assessing the diurnal variability in g_i independently and on testing whether variable diurnal g_i significantly improves the accuracy and precision of predictions of Δ in leaf models.

Model predictions: Δ_{comp}, $\Delta_{revised}$ and Δ_{simple}

Our study supports the use of the more comprehensive models, Δ_{comp} and $\Delta_{revised}$, that incorporate fractionations associated with the diffusion pathway and decarboxylation activity, to describe leaf Δ in our semi-arid system. The limitations of these models are that they require assumptions of the true value of fractionation during carboxylation and decarboxylation, in addition to an accurate estimate of g_i. Our sensitivity analysis showed that variation in e at low A resulted in ~9‰ variation in Δ_{ef}, emphasizing the importance of e in plants, such as juniper, that exhibit relatively

high R compared with A. Our estimate of e was based on the dark respiration fractionation, and we may have over- or underestimated the true value of e or R_d and introduced model error. However, we have shown that both models produced similar errors in their predictions of Δ.

The importance of decarboxylation activity in juniper Δ is reflected both in the e^* values we calculated and the Δ_{ef} estimates obtained from g_i plots. We calculated e^* values ranging from –12.5 to +1.2‰, values that suggest the isotopic disequilibria between recent photosynthate and the respiratory substrate being utilized was, at times, substantial. Further, our Δ_{ef} estimates were mostly between –6.9 and 0‰, whereas previous observations were close to 0‰ (Evans *et al.* 1986). It is also possible that other factors, such as stomatal patchiness, may not be fully captured in our estimates of p_i, which could alter the p_i/p_a ratio important to all of the Δ models (Farquhar 1989).

Despite lacking decarboxylation and g_i components, Δ_{simple} outperformed the more comprehensive models in June. Further, Δ_{simple} exhibited modest error in predicting Δ_{obs} compared with Δ_{comp} and $\Delta_{revised}$ in July and August, but consistently overestimated Δ_{obs}, predicting Δ values whose mean difference were >1.0‰ above Δ_{obs} in all 3 months. This may represent a larger systematic bias than that exists in the other models, although utilizing a lower b value reduced model bias while moderately increasing error. However, all of the models exhibited non-trivial RMSE, ranging from 1.5 to 3.2‰, suggesting that a significant amount of variability remains to be captured. Future field studies should aim to independently estimate the variability in diurnal Δ_{ef} and g_i to ascertain their impacts on diurnal leaf isotopic exchange. Similarly, future controlled studies should partition the net flux to assess g_i and Δ_{ef}, as well as the regulatory influence of environmental variables, such as temperature and PPFD, on these components of carbon discrimination.

CONCLUSIONS

Our study demonstrates that the diurnal variation in Δ in our semi-arid conifer ecosystem was of similar trend and magnitude to that observed in ecosystems as diverse as tropical forest and mesic conifer forest. Additionally, we demonstrated that Δ varies rapidly in response to shifts in environmental conditions, and that the comprehensive Farquhar *et al.* (1982) model and its descendents are capable of capturing a wide range of diurnal variation in leaf Δ. Our observations are consistent with previous results showing low Δ during conditions of low soil water availability and elevated VPD and PPFD, and higher Δ when soil water was more abundant, PPFD was variable, and VPD was low. We observed a linear relationship between Δ and p_i/p_a in June, but found a strong curvilinear relationship in July and August. Future studies might be strengthened by testing this relationship in other species over a wide range of p_i/p_a and environmental conditions. Our findings support the inclusion of g_i and decarboxylation activity to attain the most accurate and precise predictions of Δ from leaf models, and evolving technologies, such as TDL, make these improvements more easily achievable. Lastly, the magnitude of diurnal variation in g_i of other C_3 species needs to be quantified, as do the environmental and physiological drivers of this variation, so that g_i can be more accurately parameterized in future ecosystem process models.

ACKNOWLEDGMENTS

We thank H. Powers, K. Brown and C. Meyer for extensive technical support, and the Institute of Geophysics and Planetary Physics at Los Alamos National Laboratory (project 95566-001-05), the National Science Foundation (IOS-0719118), UNM PIBBS and the UNM Biology Department Lynn A. Hertel Graduate Research Award for funding. We also thank Professor Graham Farquhar and two anonymous reviewers for their comments that improved the paper.

REFERENCES

Atkin O.K., Evans J.R., Ball M.C., Lambers H. & Pons T.L. (2000) Leaf respiration of snow gum in the light and dark. Interactions between temperature and irradiance. *Plant Physiology* **122,** 915–923.

Atkin O.K., Bruhn D., Hurry V.M. & Tjoelker M.G. (2005) The hot and the cold: unravelling the variable response of plant respiration to temperature. *Functional Plant Biology* **32,** 87–105.

Baldocchi D.D. & Bowling D.R. (2003) Modelling the discrimination of $^{13}CO_2$ above and within a temperate broad-leaved forest canopy on hourly to seasonal time scales. *Plant, Cell & Environment* **26,** 231–244.

Barbour M.M., Hunt J.E., Dungan R.J., Turnbull M.H., Brailsford G.W., Farquhar G.D. & Whitehead D. (2005) Variation in the degree of coupling between $\delta^{13}C$ of phloem sap and ecosystem respiration in two *Nothofagus* forests. *New Phytologist* **166,** 497–512.

Barbour M.M., McDowell N.G., Tcherkez G., Bickford C.P. & Hanson D.T. (2007a) A new measurement technique reveals rapid post-illumination changes in the carbon isotope composition of leaf-respired CO_2. *Plant, Cell & Environment* **30,** 469–482.

Barbour M.M., Farquhar G.D., Hanson D.T., Bickford C.P., Powers H. & McDowell N.G. (2007b) A new measurement technique reveals temporal variation in $\delta^{18}O$ of leaf-respired CO_2. *Plant, Cell & Environment* **30,** 456–468.

Bernacchi C.J., Portis A.R., Nakano H., von Caemmerer S. & Long S.P. (2002) Temperature response of mesophyll conductance. Implications for the determination of rubisco enzyme kinetics and for limitations to photosynthesis in vivo. *Plant Physiology* **130,** 1992–1998.

Bowling D.R., McDowell N.G., Bond B.J., Law B.E. & Ehleringer J.R. (2002) ^{13}C content of ecosystem respiration is linked to precipitation and vapor pressure deficit. *Oecologia* **131,** 113–124.

Bowling D.R., Sargent S.D., Tanner B.D. & Ehleringer J.R. (2003) Tunable diode laser absorption spectroscopy for stable isotope studies of ecosystem-atmosphere CO_2 exchange. *Agricultural and Forest Meteorology* **118,** 1–19.

Bowling D.R., Pataki D.E. & Randerson J.T. (2008) Carbon isotopes in terrestrial ecosystem pools and CO_2 fluxes. *New Phytologist Tansley Review* **178,** 24–40.

Breshears D.D. (2008) Structure and function of woodland mosaics: consequences of patch-scale heterogeneity and connectivity along the grassland-forest continuum. In *Western North American Juniperus Woodlands – A Dynamic Vegetation Type* (ed. O.W. Van Auken), pp. 58–92. Springer, New York, NY, USA.

Brooks A. & Farquhar G.D. (1985) Effect of temperature on the CO_2/O_2 specificity of ribulose-1,5-bisphosphate carboxylase/oxygenase and the rate of respiration in the light. *Planta* **165,** 397–406.

Brooks J.R., Flanagan L.B., Buchmann N. & Ehleringer J.R. (1997) Carbon isotope composition of boreal plants: functional grouping of life forms. *Oecologia* **110,** 301–311.

Brugnoli E. & Farquhar G.D. (2000) Photosynthetic fractionation of carbon isotopes. In *Photosynthesis: Physiology and Metabolism* (eds R.C. Leegood, T.D. Sharkey & S. von Caemmerer), pp. 399–434. Kluwer Academic, Dordrecht, the Netherlands.

Brugnoli E., Hubick K.T., von Caemmerer S., Wong S.C. & Farquhar G.D. (1988) Correlation between the carbon isotope discrimination in leaf starch and sugars of C_3 plants and the ratio of intercellular and atmospheric partial pressures of carbon dioxide. *Plant Physiology* **88,** 1418–1424.

von Caemmerer S. & Evans J.R. (1991) Determination of the average partial pressure of CO_2 in the chloroplasts from leaves of several C_3 plants. *Australian Journal of Plant Physiology* **18,** 287–305.

Chen B. & Chen J.M. (2007) Diurnal, seasonal and interannual variability of carbon isotope discrimination at the canopy level in response to environmental factors in a boreal forest ecosystem. *Plant, Cell & Environment* **30,** 1223–1239.

Ciais P., Tans P.P., Trolier M., White J.W.C. & Francey R.J. (1995) A large northern hemisphere terrestrial CO_2 sink indicated by the $^{13}C/^{12}C$ ratio of atmospheric CO_2. *Science* **269,** 1098–1102.

Davenport D.W., Wilcox B.P. & Breshears D.D. (1996) Soil morphology of canopy and inter-canopy sites in a pinon-juniper woodland. *Soil Science Society of America Journal* **60,** 1881–1887.

Davison A.C. & Hinkley D.V. (1997) *Bootstrap Methods and Their Application*. Cambridge University Press, New York, NY, USA.

De Lucia E.H., Whitehead D. & Clearwater M.J. (2003) The relative limitation of photosynthesis by mesophyll conductance in co-occurring species in a temperate rainforest dominated by a conifer *Dacrydium cupressinum*. *Functional Plant Biology* **30,** 1197–1204.

Delfine S., Alvino A., Villani M.C. & Loreto F. (1999) Restrictions to carbon dioxide conductance and photosynthesis in spinach leaves recovering from salt stress. *Plant Physiology* **119,** 1101–1106.

Diaz-Espejo A., Nicolás E. & Fernandez J.E. (2007) Seasonal evolution of diffusional limitations and photosynthetic capacity in olive under drought. *Plant, Cell & Environment* **30,** 922–933.

Duranceau M., Ghashghaie J., Badeck F., Deleens E. & Cornic G. (1999) $\delta^{13}C$ of CO_2 respired in the dark in relation to $\delta^{13}C$ of leaf carbohydrates in *Phaseolus vulgaris* L. under progressive drought. *Plant, Cell & Environment* **22,** 515–523.

Ehleringer J.R. (1993) Variation in leaf carbon isotope discrimination in *Encelia farinosa*: implications for growth, competition, and drought survival. *Oecologia* **95,** 340–346.

Ehleringer J.R., Phillips S.L. & Comstock J.P. (1992) Seasonal variation in the carbon isotopic composition of desert plants. *Functional Ecology* **6,** 396–404.

Ethier G.J., Livingston N.J., Harrison D.L., Black T.A. & Moran J.A. (2006) Low stomatal and internal conductance to CO_2 versus Rubisco deactivation as determinants of the photosynthetic decline of ageing evergreen leaves. *Plant, Cell & Environment* **29,** 2168–2184.

Evans J.R., Sharkey T.D., Berry J.A. & Farquhar G.D. (1986) Carbon isotope discrimination measured concurrently with gas exchange to investigate CO_2 diffusion in leaves of higher plants. *Australian Journal of Plant Physiology* **13,** 281–292.

Farquhar G.D. (1989) Models of integrated photosynthesis of cells and leaves. *Philosophical Transactions of the Royal Society of London. Series B, Biological Sciences* **323,** 357–367.

Farquhar G.D. & Richards R.A. (1984) Isotopic composition of plant carbon correlates with water-use efficiency of wheat genotypes. *Australian Journal of Plant Physiology* **11,** 539–552.

Farquhar G.D. & Sharkey T.D. (1982) Stomatal conductance and photosynthesis. *Annual Review of Plant Physiology* **33,** 317–345.

Farquhar G.D., von Caemmerer S. & Berry J.A. (1980) A biochemical model of photosynthetic CO_2 assimilation in leaves of C_3 species. *Planta* **149,** 78–90.

Farquhar G.D., O'Leary M.H. & Berry J.A. (1982a) On the relationship between carbon isotope discrimination and the intercellular carbon dioxide concentration in leaves. *Australian Journal of Plant Physiology* **9,** 121–137.

Farquhar G.D., Ball M.C., von Caemmerer S. & Roksandic Z. (1982b) Effect of salinity and humidity on $\delta^{13}C$ value of halophytes – evidence for diffusional isotope fractionation determined by the ratio of intercellular/atmospheric partial pressure of CO_2 under different environmental conditions. *Oecologia* **52,** 121–124.

Farquhar G.D., Ehleringer J.R. & Hubick K.T. (1989) Carbon isotope discrimination and photosynthesis. *Annual Review of Plant Physiology and Plant Molecular Biology* **40,** 503–537.

Flexas J., Ribas-Carbo M., Hanson D.T., Bota J., Otto B., Cifre J., McDowell N., Medrano H. & Kaldenhoff R. (2006) Tobacco aquaporin NtAQP1 is involved in mesophyll conductance to CO_2 in vivo. *The Plant Journal* **48,** 427–439.

Flexas J., Diaz-Espejo A., Galmés J., Kaldenhoff R., Medrano H. & Ribas-Carbo M. (2007) Rapid variations of mesophyll conductance in response to changes in CO_2 concentration around leaves. *Plant, Cell & Environment* **30,** 1284–1298.

Galmés J., Medrano H. & Flexas J. (2007) Photosynthetic limitations in response to water stress and recovery in Mediterranean plants with different growth forms. *New Phytologist* **175,** 81–93.

Gessler A., Tcherkez G., Peuke A.D., Ghashghaie J. & Farquhar G.D. (2008) Experimental evidence for diel variations of the carbon isotope composition in leaf, stem and phloem sap organic matter in *Ricinus communis*. *Plant, Cell & Environment* **31,** 941–953. doi: 10.1111/j.1365-3040.2008.01806.x.

Ghashghaie J., Duranceau M., Badeck F.-W., Cornic G., Adeline M.-T. & Deleens E. (2001) $\delta^{13}C$ of CO_2 respired in the dark in relation to $\delta^{13}C$ of leaf metabolites: comparison between *Nicotiana sylvestris* and *Helianthus annuus* under drought. *Plant, Cell & Environment* **24,** 505–515.

Ghashghaie J., Badeck F.W., Lanigan G., Nogues S., Tcherkez G., Deleens E., Cornic G. & Griffiths H. (2003) Carbon isotope fractionation during dark respiration and photorespiration in C_3 plants. *Phytochemistry Reviews* **2,** 145–161.

Gillon J.S. & Griffiths H. (1997) The influence of (photo)respiration on carbon isotope discrimination in plants. *Plant, Cell & Environment* **20,** 1217–1230.

Grassi G. & Magnani F. (2005) Stomatal, mesophyll conductance and biochemical limitations to photosynthesis as affected by drought and leaf ontogeny in ash and oak trees. *Plant, Cell & Environment* **28,** 834–849.

Griffis T.J., Baker J.M., Sargent S.D., Tanner B.D. & Zhang J. (2004) Measuring field-scale isotopic CO_2 fluxes with tunable diode laser absorption spectroscopy and micrometeorological techniques. *Agricultural and Forest Meteorology* **124,** 15–29.

Hanba Y., Shibasaka M., Hayashi Y., Hayakawa T., Kasamo K., Terashima I. & Katuhara M. (2006) Overexpression of the barley aquaporin HvPIP2;1 increases internal CO_2 conductance and CO_2 assimilation in the leaves of transgenic rice plants. *Plant and Cell Physiology* **47**(Suppl.), S24–S24.

Harwood K.G., Gillon J.S., Griffiths H. & Broadmeadows M.S.J. (1998) Diurnal variation of $\Delta^{13}CO_2$, $\Delta C^{18}O^{16}O$ and evaporative site enrichment of $\delta H_2{}^{18}O$ in *Piper aduncum* under field conditions in Trinidad. *Plant, Cell & Environment* **21,** 269–283.

Hymus G.J., Maseyk K., Valentini R. & Yakir D. (2005) Large daily variation in ^{13}C-enrichment of leaf-respired CO_2 in two *Quercus* forest canopies. *New Phytologist* **167,** 377–384.

Jordan D.B. & Ogren W.L. (1984) The CO_2/O_2 specificity of ribulose 1,5 bisphosphate carboxylase/oxygenase. Dependence on ribulosebisphosphate concentration, pH, and temperature. *Planta* **161,** 308–313.

Knohl A., Werner R.A., Brand W.A. & Buchmann N. (2005) Short-term variations in ecosystem $\delta^{13}C$ of ecosystem respiration reveals link between assimilation and respiration in a deciduous forest. *Oecologia* **142,** 72–80.

Kozaki A. & Takeba G. (1996) Photorespiration protects C_3 plants from photooxidation. *Nature* **384,** 557–560.

Ku S.-B. & Edwards G.E. (1977) Oxygen inhibition of photosynthesis II. Kinetic characteristics as affected by temperature. *Plant Physiology* **59,** 991–999.

Lloyd J., Syvertsen J.P., Kriedemann P.E. & Farquhar G.D. (1992) Low conductances for CO_2 diffusion from stomata to the sites of carboxylation in leaves of woody species. *Plant, Cell & Environment* **15,** 873–899.

McDowell N.G., Bowling D.R., Schauer A., Irvine J., Bond B.J., Law B.E. & Ehleringer J.R. (2004) Associations between carbon isotope ratios of ecosystem respiration, water availability, and canopy conductance. *Global Change Biology* **10,** 1767–1784.

McDowell N., Baldocchi D., Barbour M., *et al.* (2008a) Measuring and modeling the stable isotope composition of biosphere-atmosphere CO_2 exchange: where are we and where are we going? *EOS* **89,** 94–95.

McDowell N.G., Pockman W.T., Allen C., *et al.* (2008b) Mechanisms of plant survival and mortality during drought: why do some plants survive while others succumb to drought? *New Phytologist Tansley Review* **178,** 719–739.

O'Leary M.H. (1981) Carbon isotope fractionation in plants. *Phytochemistry* **20,** 553–567.

Prater J.L., Mortazavi B. & Chanton J.P. (2005) Diurnal variation of the $\delta^{13}C$ of pine needle respired CO_2 evolved in darkness. *Plant, Cell & Environment* **29,** 202–211.

R Core Development Team (2008) R: A Language and Environment for Statistical Computing. R Foundation for Statistical Computing, Vienna. Austria. ISBN 3-900051-07-0. Available at: http://www.R-project.org (accessed 24 February 2009).

Randerson J.T., Masiello C.A., Still C.J., Rahn T., Poorter H. & Field C.B. (2006) Is carbon within the global terrestrial biosphere becoming more oxidized? Implications for trends in atmospheric O-2. *Global Change Biology* **12,** 260–271.

Roeske C.A. & O'Leary M.H. (1984) Carbon isotope effects on the enzyme-catalyzed carboxylation of ribulose bisphosphate. *Biochemistry* **23,** 6275–6284.

Rooney M.A. (1988) *Short-term carbon isotopic fractionation in plants*. PhD thesis, University of Wisconsin-Madison.

Sharkey T.D., Bernacchi C.J., Farquhar G.D. & Singsaas E.L. (2007) In practice: fitting photosynthetic response curves for C_3 leaves. *Plant, Cell & Environment* **30,** 1035–1040.

Smith B.N. & Epstein S. (1971) Two categories of $^{13}C/^{12}C$ ratios for higher plants. *Plant Physiology* **47,** 380–384.

Tcherkez G. (2006) How large is the carbon isotope fractionation of the photorespiratory enzyme glycine decarboxylase? *Functional Plant Biology* **33,** 911–920.

Tcherkez G., Nogues S., Bleton J., Cornic G., Badeck F. & Ghashghaie J. (2003) Metabolic origin of carbon isotope composition of leaf dark-respired CO_2 in French Bean. *Plant Physiology* **131,** 237–244.

Tcherkez G., Cornic G., Bligny R., Gout E. & Ghashghaie J. (2005) In vivo respiratory metabolism of illuminated leaves. *Plant Physiology* **138,** 1596–1606.

Tcherkez G., Bligny R., Gout E., Mahé A., Hodges M. & Cornic G. (2008) Respiratory metabolism of illuminated leaves depends on CO_2 and O_2 conditions. *Proceedings of the National Academy of Sciences of the United States of America* **105,** 797–802.

Tu K. & Dawson T. (2005) Partitioning ecosystem respiration using stable carbon isotope analyses of CO_2. In *Stable Isotopes and Biosphere–Atmosphere Interactions: Processes and Biological Controls* (eds L.B. Flanagan, J.R. Ehleringer & D.E. Pataki), pp. 125–148. Elsevier Academic Press, Great Britain, UK.

Uehlein N., Otto B., Hanson D.T., Fischer M., McDowell N. & Kaldenhoff R. (2008) Function of *Nicotiana tabacum* aquaporins as chloroplast gas challenges the concept of membrane CO_2 permeability. *The Plant Cell* **20,** 648–657.

Warren C.R. & Dreyer E. (2006) Temperature response of photosynthesis and internal conductance to CO_2: results from two independent approaches. *Journal of Experimental Botany* **12,** 3057–3067.

Warren C.R., Ethier G.J., Livingston N.J., Grant N.J., Turpin D.H., Harrison D.L. & Black T.A. (2003) Transfer conductance in second growth Douglas-fir (*Pseudotsuga menziesii* (Mirb.) Franco) canopies. *Plant, Cell & Environment* **26,** 1215–1227.

Warren C.R., Livingston N.J. & Turpin D.H. (2004) Water stress decreases the transfer conductance of Douglas-fir (*Pseudotsuga menziesii*) seedlings. *Tree Physiology* **24,** 971–979.

Wingate L., Seibt U., Moncrieff J.B., Jarvis P.G. & Lloyd J. (2007) Variations in ^{13}C discrimination during CO_2 exchange by *Picea sitchensis* branches in the field. *Plant, Cell & Environment* **30,** 600–616.

Yakir D. (2003) The stable isotope composition of atmospheric CO2. In *Treatise on Geochemistry* Vol. 4 (ed. R.L. Rudnick), pp. 175–212. Elsevier Press, San Diego, CA, USA.

Yamori W., Noguchi K., Hanba Y.T. & Terashima I. (2006) Effects of internal conductance on the temperature dependence of the photosynthetic rate in spinach leaves from contrasting growth temperatures. *Plant Cell Physiology* **47,** 1069–1080.

Received 8 October 2008; received in revised form 23 January 2009; accepted for publication 27 January 2009